PROCEEDINGS OF SPIE

SPIEDigitalLibrary.org/conference-proceedings-of-spie

Combined multi-protocols qMRI for thigh muscle analysis: a preliminary study

Mehran Azimbagirad, Guillaume Dardenne, Douraied Ben Salem, Olivier Remy-Neris, Valerie Burdin

Mehran Azimbagirad, Guillaume Dardenne, Douraied Ben Salem M.D., Olivier Remy-Neris, Valerie Burdin, "Combined multi-protocols qMRI for thigh muscle analysis: a preliminary study," Proc. SPIE 12088, 17th International Symposium on Medical Information Processing and Analysis, 120880G (10 December 2021); doi: 10.1117/12.2604236

SPIE.

Event: Seventeenth International Symposium on Medical Information Processing and Analysis, 2021, Campinas, Brazil

Combined Multi-Protocols qMRI for Thigh Muscle Analysis: A Preliminary Study

Mehran Azimbagirad[a,d], Guillaume Dardenne[b,d], Douraied Ben Salem[a,b,d], Olivier Rémy-Néris[a,b,d], and Valérie Burdin[c,d]

[a]University of Western Brittany (UBO), Brest, France;
[b]University Hospital of Brest, France;
[c]IMT Atlantique, Institut Mines Telecom, Brest, France;
[d]INSERM UMR 1101 LaTIM, Brest, France.

ABSTRACT

Quantitative MRI (qMRI) has been shown to be crucial for assessing organ dysfunction in the body. Usually, in qMRI approaches, a few metrics are extracted to distinguish normal and abnormal tissues. In this study, we coupled four MRI protocols (mDIXON T1, T1 and T2 mapping and DTI) to obtain 34 complementary metrics including 20 shape metrics, 2 texture metrics and 12 water diffusivity metrics for thigh muscle analysis. These metrics were calculated on both thighs to detect a pathological difference between a pair of right and left muscles. The method is based on a dimension reduction method and a projection of shape and diffusivity metrics into a three-dimensional linear latent space, along with two texture metrics. 5 healthy individuals (10 thighs, each thigh 7 muscles, i.e., 4 flexors and 3 extensors) were scanned to provide the reference scores. The developed pipeline was used to analyse the pair thighs of 4 patients in order to suggest a specific muscle therapy before total knee arthroplasty (TKA) individually for each of the 7 muscles. Preliminary results from the analysis of thigh muscle texture, shape and diffusivity showed that this qMRI protocol can help to suggest a targeted, patient-specific exercise plan to improve muscle recovery after TKA surgery. More healthy and pathological subjects are needed to confirm these encouraging results.

Keywords: qMRI, thigh muscles analysis, Principal Component Analysis

1. INTRODUCTION

Several tools have been developed and used to extract clinical parameters to assess and monitor muscle disease[1] such as, Ultrasonography,[2] anthropometric assessment[3] and bioelectrical impedance analysis.[4] Nevertheless, most of such tools are employed to analyse the thigh muscles globally and not individually. Besides, Magnetic Resonance Imaging (MRI) is a non-invasive tool to estimate thigh muscle volume, fat proportion and several other metrics, individually, as the most reliable technique.[5] Thus, MRI has been used as a crucial tool to either diagnose or follow up the muscle disorders. This technique is able to extract several metrics to differentiate characteristic of normal and fatty infiltration of muscles.[6] There are numerous studies investigating the correlation between such metrics (extracted from muscle's MRI) and muscle diseases such as muscular dystrophy,[7] Congenital myopathies,[8] myasthenia gravis and Graves' orbitopathy.[9]

In quantitative MRI (qMRI) of muscle disorder studies, usually one or more protocols can be used to extract the metrics. For example, Dixon, T1 and T2-weighted sequences allowed establishment of the pattern, texture and anatomical distribution of muscular degeneration while DTI is employed to provide information about diffusivity of water in muscle tissues (see Fig. 1). MRI protocols are chosen respect to the physical/chemical properties of the scanned tissues to detect abnormalities. Therefore, for each protocol, the extracted parameters may differ and interpret individually.

M.A: correspondence author, E-mail: mehran.azimbagirad@univ-brest.fr, Address:22 Av Camille Desmoulins, 29200 Brest, France, ,Telephone: 33-02303-3837
G.D: E-mail:guillaume.dardenne@univ-brest.fr,
D.B.S: E-mail:douraied.bensalem@chu-brest.fr
O.R.N: E-mail:olivier.remy-neris@univ-brest.fr
V.B: E-mail: valerie.burdin@imt-atlantique.fr

17th International Symposium on Medical Information Processing and Analysis, edited by Eduardo Romero Eduardo Tavares Costa, Jorge Brieva, Leticia Rittner, Marius George Linguraru, Natasha Lepore
Proc. of SPIE, Vol. 12088, 120880G · © 2021 SPIE · 0277-786X · doi: 10.1117/12.2604236

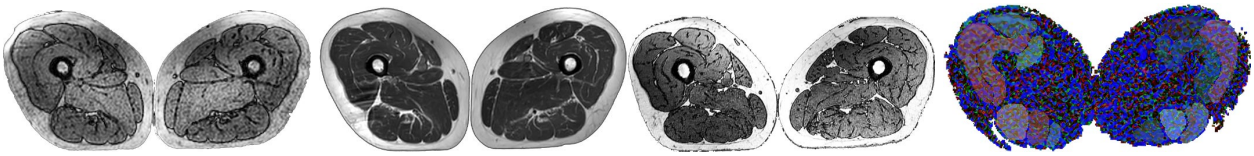

(a) T1 (b) T2 (c) DIXON (d) DTI

Figure 1. A cross-section of four MRI protocols for thigh muscle analysis. a) is T1, b) T2, c) DIXON protocol (out of phase) and d) DTI or diffusion Tensor model using weighted least squares which takes into account the noise characteristics of the MRI images to weight the DWI samples based on their intensity magnitude. Several metrics can be extracted from the Tensor model.

Several studies have been investigating such protocols as Sproule et al.[10] which used T1-weighted protocol to estimate the volume of muscle as a metric for spinal muscle atrophy analysis. Another example is a study in which they used Dixon protocol to extract fat fraction as a metric.[11] As an example of multi-MRI protocols usage on thigh muscles analysis, we refer to T1-T2-Dixon by Fischmann et al.[12] in which they examined 8 patients diagnosed by Oculopharyngeal muscular dystrophy and 5 healthy subjects to compare the MRI metrics. As another multi-protocol analysis, i.e., T1-DTI, Charles et al.[13] provided an architecture data set of 20 lower limb muscles from 10 healthy adults. They found that maximum isometric force and muscle fiber lengths were found not to scale with subject anthropometry, suggesting that these factors may be difficult to predict using scaling or optimization algorithms. Last but not least, we refer to a T2-DTI-Dixon analysis by Monte et al.[14] in which they examined 5 DTI metrics, i.e., three eigen values, mean diffusivity and fractional anisotropy. Their analysis showed good repeatability of all DTI parameters except fractional anisotropy which might be susceptible to signal to noise ratio.

On the other hand, in qMRI approaches using a protocol, several metrics can be extracted from the same protocol. For instance, in T1-weighted protocol, in addition to T1 value, volume metric, Fat fraction can also be provided. More specifically in DTI protocol, over than 13 metrics[15] can be extracted such as Fractional Anisotropy, Apparent Diffusivity Coefficient, Parallel diffusivity, perpendicular diffusivity, eigen values, mode, etc. For the most of the reviewed studies, only a few metrics were analysed while the most of them were not extracted or eliminated from the results.

Usually, the recommendation for Total knee arthroplasty (TKA) is based on a patient's pain and disability, but not specifically on their age though TKA patients are normally between 50 to 80 years old.[16] While for young patients under TKA the rehabilitation may be fast, for middle-aged or older adults it may takes a while even a year. Thus, a post and/or pre-surgical training programme may also be used to improve patients' post-surgical functional status.[17] In order to define an effective patient specific training programme, probably targeting the reinforcement of weaker muscles may boost the rehab. But to do this, an accurate assessment pipeline using qMRI is required to deeply detect abnormalities of such muscles.

For those TKA patients that only one knee goes under surgery, it might be possible to detect abnormal muscle according to compare right-left thigh muscle MRI metrics and the thigh which includes in surgery. In our best knowledge, this is the first study where we used a T1-T2-Dixon-DTI protocols to extract 34 metrics in three groups of Texture, shape and diffusivity analysis of thigh muscles for a control group. Then using principal component analysis, we provided the mean components (by different weights) as reference scores. Later these scores are used to detect abnormal thigh muscle for TKA patient. According to the abnormal muscles, a patient-specific exercise programme can be suggested to improve the rehabilitation.

Sec. 2 describes the overall extracting metrics of four MRI protocols for thigh muscles as well as providing reference scores for the metric. Sec. 3 is dedicated to the experiments on 70 normal muscles from 10 healthy thighs and 56 muscles from four TKA patients and results. A discussion and a conclusion complete this paper in Sec. 4 and Sec. 5, respectively.

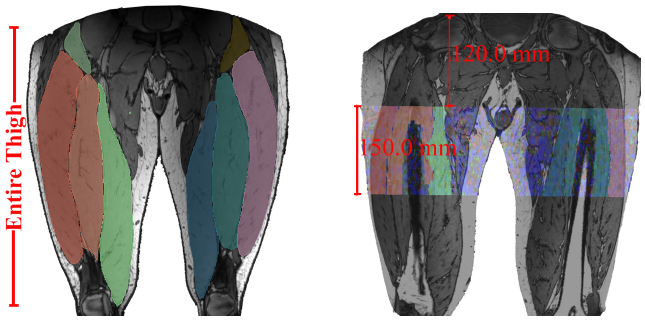

(a) FOV for DIXON (b) FOV for T1,T2 & DTI

Figure 2. Field of view of the selected part of the thigh muscles acquisitions for a) DIXON protocol , and b) T1, T2 and DTI protocols, in coronal view. The resolution for each protocol is different according to its extracting metric methods.

2. METHOD

2.1 Subjects and qMRI protocols

According to the Declaration of Helsinki with ethical approval protocol (n° 2019-A01703-54), 10 entire thighs from 5 healthy volunteers with an average age of 48 years (±10) were scanned. In addition, 4 patients under TKA were included in three steps: before exercise, before surgery and after surgery (each step at one month intervals). Both acquisitions (healthy and patient subjects) were performed using a 3.0 Tesla scanner Philips, Elition X (Best, Netherlands) with modified Dixon three-dimensional (3D) T1-weighted (T1W) gradient echo technique (mDixon-3D-GRE), allowing fat (F)–water(W) separation and a voxel resolution of $0.5 \times 0.5 \times 1.0\ mm^3$ (see Fig. 2 (a)). For T1 map we used Modified Look-Locker inversion recovery (MOLLI) protocol with flip angle = 20° in 8 echos (Time Inversion in ms) as: 116, 350, 1116, 1350, 2116, 2350, 3116 and 4116. For T2 map we used T2 Turbo Spine Echo protocol, with flip angles = 90°, 4.9 ms interval with 9 echo times. For DTI we used smart shim protocol with 16 directions plus the B0. The field of view (FOV) of T1-T2 mapping and DTI scanning can be seen in Fig. 2 (b) with a voxel resolution of $1.5 \times 1.5 \times 5.0\ mm^3$. Two groups of thigh muscles were selected to evaluate the pipeline: the quadriceps Femoris muscles (Rectus Femoris (RF), Vastus Lateralis (VL), Vastus Intermedius (VI), Vastus Medialis (VM)), and the Hamstrings muscles (Biceps Short Head (BSH), Semitendinosus (ST), Semimembranosus (SM)).

We used the 3D Slicer software[15] to entirely label seven thigh muscles (see Fig. 2).

2.2 Metrics extraction

2.2.1 Shape metrics

For the control group, using Dixon image (Out of Phase) and the label map of the muscles, we were able to compare each of the right thigh muscles to the left ones. Therefore, we have to mirror the left muscles (e.g., RF_L for the left rectus femoris) and register to the corresponding muscle in the right side (i.e., RF_R). We used a rigid approach (6 degrees of freedom) for this aim. Later, we extracted 20 shape metrics: Dice Coefficient (DICE), Jaccard Coefficient (JACRD), Area under ROC Curve (AUC), Cohen Kappa (KAPPA), Rand Index (RNDIND), Adjusted Rand Index (ADJRIND), Interclass Correlation (ICCORR), Volumetric Similarity Coefficient (VOLSMTY), Hausdorff distance (HDRFDST), average distance (AVGDIST),Mahanabolis Distance (MAHLNBS), Variation of Information (VARINFO), Global Consistency Error (GCOERR), Probabilistic Distance (PROBDST), Sensitivity or Recall true positive rate (SNSVTY), Specificity or true negative rate (SPCFTY), Precision (PRCISON), F-Measure (FMEASR), Accuracy (ACURCY), Absolute Volume Difference (AVD)[18,19] by each pair muscles. These metrics indicate the similarity between left and right thigh muscles.

2.2.2 Texture metrics

In order to extract two texture metrics using T1-T2 mapping, firstly we corrected the bias field effect. Later, we extracted a mean intensity of each thigh muscle (in the labeled region) for each echo. Both first echos of

T1-mapping and T2-mapping were removed and left the 6 mean values as y_1 for T1 and 7 as y_2 for T2, we fit an exponential function to estimate the T1 and T2 values for each muscle, respectively, as following:

$$y_1 = A - B\, e^{(-\frac{TI}{T1})}, \tag{1}$$

where TI is the Time Inversion (ms) and

$$y_2 = C\, e^{(-\frac{ET}{T2})} + D, \tag{2}$$

where ET is the Echo Time (ms). Therefore, for each muscle (the region of labeled muscle), the average of T1 value is called as a texture metric as well as T2 value.

2.2.3 Water diffusivity metrics

Using DTI protocol and the label of each muscle, we extract 12 water diffusivity metrics: Fractional Anisotropy, Trace, Determinant, Relative Anisotropy, Mode, Linear Measure, Planar Measure, Spherical Measure, Parallel Diffusivity, Perpendicular Diffusivity, Apparent Diffusivity Coefficient, and Maximum eigen value of control group. Each metric considers one aspect of water diffusivity inside the muscles (e.g., see Fig. 3). In order to normalize all metrics, we scaled them to an interval $[0, 1]$.

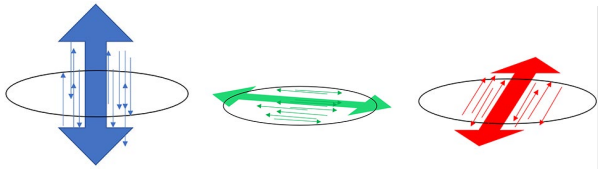

(a) (b) (c)

Figure 3. Three different directions for water diffusivity inside the muscle which can be estimated using DTI protocol. a) top-bottom b) right-left, c) back-front. However, it is possible to extract over than 30 directions water diffusivity for only one voxel.

2.3 Reference scores

We want to provide healthy scores for non pathologic thigh muscle using Shape-Texture-Diffusivity metrics. Firstly, for both Shape and Diffusivity metrics, we decrease the dimension using a principal component analysis (PCA). Then, we introduce four reference scores for thigh muscle evaluation in three families as follows.

2.3.1 Shape reference scores

Since we provided 20 shape metrics for each m thigh muscle, we suggested to use PCA to reduce the redundancy. The PCA analysis gives the mean vector ($\bar{C}_m = [\bar{c}_1, \bar{c}_2, \bar{c}_3, \bar{c}_4]$, we removed the last component which had a weight $< 0.1\%$), the feature eigenvector components FVC_m and the associated eigenvalues (weighted or W_m) for each muscle m. For example, for the Vastus Intermedius muscle (m =VI), 20 shape metrics are provided using 5 control subjects called Shape metric vectors VI_1 to VI_5 (Fig. 4). For each muscle m, to obtain its components vector in the 3D latent space, ($C^i_m = [c^i_1, c^i_2, c^i_3]$, $i = 1, \ldots, 5$) we used:

$$C^i_m = m_i \times FVC_m = [c^i_1, c^i_2, c^i_3], \tag{3}$$

where m_i is the shape metrics vector for the m muscle of subject i, and FVC_m is the feature vector coefficients. In order to define a reference score (the maximum distance allowed from $\bar{C}_m$ to say that the muscle m is normal with no controlateral difference), we measured the weighted distance between $\bar{C}_m$ and C^i_m (the component vector of each healthy subject) as:

$$d^i_m(C^i_m, \bar{C}) = [(c^i_1 - \bar{c}_1)^2 \quad (c^i_2 - \bar{c}_2)^2 \quad (c^i_3 - \bar{c}_3)^2] \begin{bmatrix} w_1 \\ w_2 \\ w_3 \end{bmatrix}, \qquad i = 1, \ldots, 5 \tag{4}$$

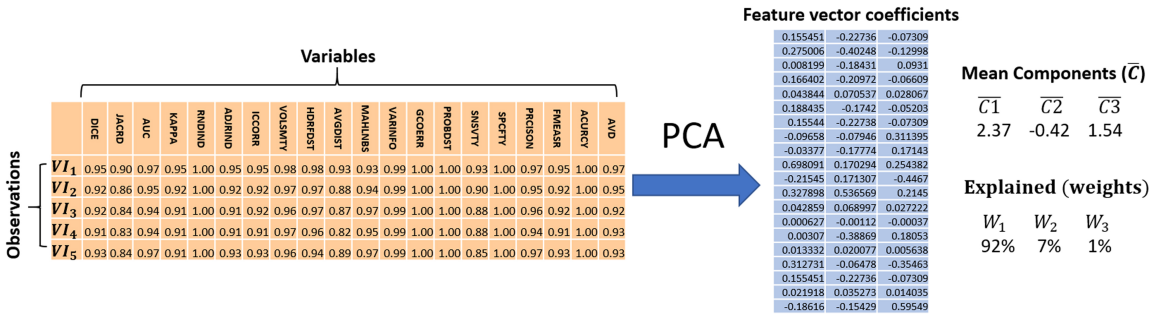

Figure 4. An example of Principal Component Analysis. VI_1 to VI_5 are the Vastus Intermedius muscle of 5 control subjects with similarity metrics between right and left VIs. $\bar{C}$= mean of components, W=weights or explained.

where w_i is the weight (explained) of component i in the PCA decomposition. Therefore, the maximum weighted distance is introduced as a Shape reference score ($Shape_{\text{ref}}$) to detect unbalance (abnormal) muscle. Thus, for the Vastus Intermedius, m =VI, the Shape reference is estimated as following:

$$Shape_{\text{ref}}(\text{VI}) = \max_i d^i_{\text{VI}}, \qquad i = 1, \ldots, 5 \tag{5}$$

This process was repeated for the other thigh muscles to provide all references for the shape metrics.

2.3.2 DTI Reference scores

We do the same process as for the shape metrics on the 12 DTI metrics to extract the mean components and the diffusivity reference scores (DTI_{ref}) for all muscles individually. For example, a reference score of the muscle VI is the maximum distance among healthy subject from $\bar{C}$ extracted from PCA analysis on diffusivity metrics as:

$$DTI_{\text{ref}}(\text{VI}) = \max_i d^i_{\text{VI}}, \qquad i = 1, \ldots, 5 \tag{6}$$

where d^i_{VI} is defined by eq.4 and C^i_m as the DTI metric components vector.

2.3.3 Texture reference scores

In order to define a texture reference score on five healthy subjects and for each muscle (e.g. VI), we average the corresponding $T1$ value and $T2$ value to extract their mean as $\overline{T1}$ and $\overline{T2}$, respectively. Then, the maximum distance to these means is defined as texture reference scores as following:

$$T1_{\text{ref}}(\text{VI}) = \max_i \|T1_i - \overline{T1}\|, \qquad i = 1, \ldots, 5 \tag{7}$$

$$T2_{\text{ref}}(\text{VI}) = \max_i \|T2_i - \overline{T2}\|, \qquad i = 1, \ldots, 5 \tag{8}$$

where $\|.\|$ represents the euclidean distance between two vectors (or absolute value of two numbers).

2.4 Abnormality detection

In order to assess patient's thigh muscles, all four protocols were used to provide the MR images. Then the suggested pipeline was used to extract the metrics and also decreased them to the components. Later, a weighted distance between the components of the patient metrics and $\bar{C}$ of control group is calculated. If this weighted distance of a muscle component is lower than the reference scores ($Shape_{ref}, DTI_{ref}, T1_{ref}$ and $T2_{ref}$), it is considered as normal, and if not, we assume that this muscle is abnormal with respect to that metric.

Consequently, the whole process from image acquisition to abnormality detection can be also seen in Fig. 5.

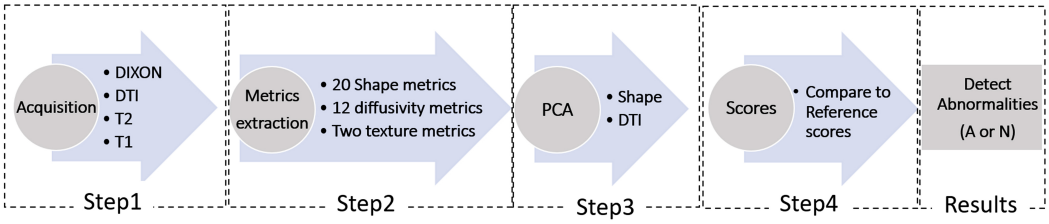

Figure 5. The pipeline process for a thigh muscle analysis: combined qMRI protocols, quantitative analysis and metrics extraction, principal component analysis and comparison to healthy subjects to detect abnormal muscles.

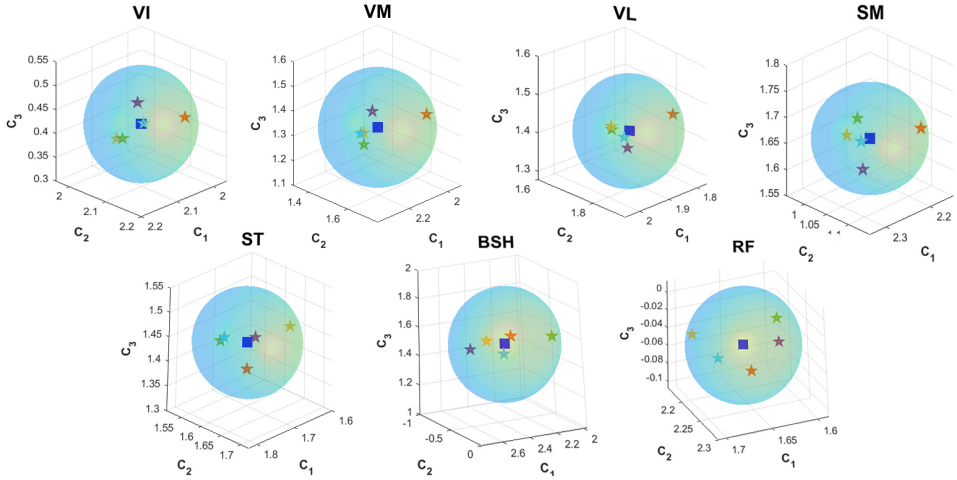

Figure 6. Using PCA on shape metrics for each thigh muscle (VI, VM, VL, SM, ST, BSH and RF), three components were extracted on five control subjects. For each muscle m, a sphere of normality is designed with a center (blue square) as the components mean $\bar{C}_m$, and a radius as the reference score for shape (eq.5). 5 colorful stars are presenting the healthy subject components.

Table 1. Calculated reference scores for abnormality detection of thigh muscles using multi-protocol Texture-Shape-Diffusivity metric analysis on 5 normal subjects.

Protocols	Reference scores	VM	VI	VL	RF	SM	ST	BSH
DIXON	$Shape_{\text{ref}}$	0.91	3.53	1.57	0.15	0.38	0.83	9.84
DTI	DTI_{ref}	0.38	1.33	1.13	1.77	0.36	0.55	0.13
T2 mapping	$T2_{\text{ref}}$	1.83	0.84	1.63	2.66	1.56	0.77	2.22
T1 mapping	$T1_{\text{ref}}$	1.83	1.12	0.64	2.41	2.64	0.84	1.02

3. RESULTS

3.1 PCA component of control group

Using the 3D slicer software, 7 muscles of 10 thighs were segmented from top to bottom on the control group. Also, 20 metrics were extracted from comparing (registering) left to right muscles. For each muscle, three PCA components were extracted as seen in Fig. 6 for the shape metric. For the control group, we estimated the thresholds for the shape, texture and diffusivity using Eq. 3 to 8 and the results can be seen in Tab. 1.

3.2 Abnormality detection using thresholds

As a trial, a patient under TKA was included in the proposed pipeline. We acquired 4 images using the MRI protocols. The muscles were segmented and all metrics for texture-shape-diffusivity were extracted. Then we used the PCA analysis to project the shape and diffusivity metrics in the 3D-latent space and we calculated the weighted distance. The results along with reference scores are presented in Tab. 2, for the patient $p = 1$. All correspondent weighted distance higher than the reference scores are considered as abnormal which can be seen in Tab. 3 on 4 TKA patients. In Tab. 3, Patient 1 in the third acquisition (P_{13}) could not stay in the MRI system to complete all acquisitions, and only Dixon was successfully acquired.

Table 2. Results of abnormality detection using the reference scores ($Shape_{\text{ref}}$, DTI_{ref}, $T2_{\text{ref}}$ and $T1_{\text{ref}}$) and a TKA patient scores ($Shape_p$, DTI_p, $T2_p$ and $T1_p$), $p = 1$.

Protocols	Scores	VM	VI	VL	RF	SM	ST	BSH
DIXON	$Shape_{\text{ref}}$	0.91	3.53	1.57	0.15	0.38	0.83	9.84
	$Shape_1$	3.86	3.83	0.65	1.12	1.94	6.55	3.97
	abnormality results*	A	A	N	A	A	A	N
DTI	DTI_{ref}	0.38	1.33	1.13	1.77	0.36	0.55	0.13
	DTI_1	0.09	0.67	0.07	0.12	0.94	0.20	0.16
	abnormality results*	N	N	N	N	A	N	A
T2 mapping	$T2_{\text{ref}}$	1.83	0.84	1.63	2.66	1.56	0.77	2.22
	$T2_1$	9.33	0.17	1.82	7.32	6.12	9.83	2.66
	abnormality results*	A	N	A	A	A	A	A
T1 mapping	$T1_{\text{ref}}$	1.83	1.12	0.64	2.41	2.64	0.84	1.02
	$T1_1$	2.12	3.47	2.58	2.26	3.62	0.82	4.04
	abnormality results*	A	A	A	N	A	N	A

* If $Shape_1 < Shape_{\text{ref}}$ then result is N=normal, else result is A=abnormal, as well as for other results.

4. DISCUSSION

qMRI studies have proven the difference between MRI metrics of normal and abnormal muscle tissues.[10–14] In this study we used 4 MRI protocols to extract 34 quantitative metrics, and then we defined reference scores using PCA analysis on the metrics. Later, for TKA patients thigh muscle analysis, the same metrics were extracted and abnormal muscles were detected using the distance between the patient metrics and the reference scores. To the best of our knowledge, it is the first study where we combined several qMRI (Dixon, T1, T2 and DTI) and different metrics aiming to introduce reference scores and abnormality detection.

Since we decreased the dimension of the metrics using PCA into 3 components, we expected the use of the mean of the components to be a reliable reference for distinguishing abnormal muscles. As you can see in Fig. 6, all components (except for BSH) are around the mean (radii are less than 0.1), showing the level of confidence of the reference scores. Besides, increasing the number of healthy subjects should improve the reliability of the reference scores.

It should be mentioned that some metrics may be less robust than others in distinguishing normal from abnormal muscles. For this purpose, we used PCA as it gives lower weights to these metrics in order to decrease their effects on the results. In addition, we used PCA component weights (w_is in equation 4) to decrease the influence of these uninformative metrics. Therefore, the mean components (as centres) and the largest distance (as radius) from these means constitute the normality space (no controlateral difference). Therefore, abnormal muscles were labelled only when their components were outside the normality sphere.

We indicated the abnormal muscles with respect to each metric between right and left side and using the reference scores. Still, one may ask which side (left or right) is abnormal. For this aim we refer to[12,14,20] which claimed that T1 and T2 values for abnormal muscles are higher than normal ones as well as DTI metrics. From the shape analysis, we could also consider that smaller volume muscle might be weaker with respect to the bigger one. According to these definitions, the first acquisition (one month before surgery) of the patients showed more abnormality for the knee under surgery. The next step in this study will be to identify which side of the body has the weakest muscles in order to provide targeted muscle therapy and to help answer the question: is it possible to pre-train these muscles in order to boost post-surgical rehabilitation?

However, the link between volume and weakness is not straightforward. In Tab. 3, apparently, some conflicts may be seen in detecting abnormal muscles using different MRI protocols. For example, the shape analysis may detect an abnormality for a muscle while DTI represent a normal status for that muscle. Besides, if a muscle is bigger, it might have more fatty tissues. Therefore, shape analysis detect that muscle as normal while DTI analysis detect it as abnormal. In fact, each of the texture, shape and diffusivity protocols separately analyses a specific functionality of muscle tissue, which may explain these conflicts.

Therefore, it is possible to find out the possible correlation between them after increasing the number of inclusions as the next step of this study. Since TKA surgery was not in priority in the recent pandemic situation (Covid-19), all the treatments postponed. Since then, the process of new inclusions is very slow but continuing. In total, 48 patients will be included in this project.

One limitation of qMRI approaches is the artifacts which take place in images such as signal to noise ratio (SNR), bias B_0 field effect, motion effect, etc. Although there are several techniques to restore information in the image, still strong artifacts may decline the correlation between MRI metrics and abnormality detection. In most of the qMRI studies that we reviewed for thigh muscles, usually moderate correlation had been found according to each MRI protocol's artifact. In our study, to conclude which metric is more reliable to detect abnormalities, more pathology subjects are needed.

There are several other metrics family such as shape based (2D and 3D), statistics, grey level cooccurence matrix, and so on which can be extracted using available tools such as PyRadiomics,[21] Matlab. Usually, such metrics are considered as Content-based image retrieval (CBIR) which normally are used in artificial neural network classifiers.[22] A big limitation of using CBIR techniques and ANN classifiers is the number of subjects to obtain an acceptance accuracy. In our study, which the number of individuals will not exceed 50, using such approaches result in bias and may not be accepted in scientific community.

5. CONCLUSION

In this study, we introduced a texture-shape-diffusivity analysis to detect abnormal thigh muscle in the clinical workflow of TKA to introduce more effective exercise programme. Firstly, we introduced a reference score of normality for 7 thigh muscles, using 5 healthy subjects, 34 metrics and four MRI protocols, i.e., T1 and T2 mapping, Dixon and DTI. The protocols are combined through a PCA analysis of the metrics. For four patients under TKA, our suggestion pipeline clustered normal/abnormal muscles with respect to each protocol. Once the proposed pipeline is evaluated on a larger number of pathological data, it will be possible to extend it to other rehabilitation schemes.

Acknowledgments

This work has benefited from a French grant managed by the National Research Agency under the "programme d'investissements d'avenir" bearing the reference ANR-17- RHUS-0005, and the financial support of the Brittany Region. Authors would like to thanks MRI technicians of Hospital of Brest, Sébastien Kerdraon, Aurelie Richard, Aurelie Turbellier and Vincent Josse for their collaboration.

REFERENCES

[1] Goebel, H. H., Sewry, C. A., and Weller, R. O., [*Muscle disease: pathology and genetics*], Wiley Online Library (2013). https://www.doi.org/10.1002/9781118635469.

[2] Washburn, N., Onishi, K., and Wang, J. H. C., "Ultrasound elastography and ultrasound tissue characterisation for tendon evaluation," *Journal of Orthopaedic Translation* **15**, 9–20 (2018).

[3] Carneiro, M. A. S., Barcelos, L. C., Nunes, P. R. P., de Souza, L. R. M. F., de Oliveira, E. P., and Orsatti, F. L., "Anthropometric equations to estimate the thigh muscle cross-sectional area by magnetic resonance imaging in young men," *Science & Sports* **34**(6), 418–421 (2019).

[4] Yamada, Y., Ikenaga, M., Takeda, N., Morimura, K., Miyoshi, N., Kiyonaga, A., Kimura, M., Higaki, Y., and Tanaka, H., "Estimation of thigh muscle cross-sectional area by single- and multifrequency segmental bioelectrical impedance analysis in the elderly," *Journal of Applied Physiology* **116**(2), 176–182 (2014).

[5] Pons, C., Borotikar, B., Garetier, M., Burdin, V., Ben Salem, D., Lempereur, M., and Brochard, S., "Quantifying skeletal muscle volume and shape in humans using mri: A systematic review of validity and reliability," *PLOS ONE* **13**(11), e0207847 (2018).

[6] Lassche, S., Küsters, B., Heerschap, A., Schyns, M. V. P., Ottenheijm, C. A. C., Voermans, N. C., and van Engelen, B. G. M., "Correlation between quantitative mri and muscle histopathology in muscle biopsies from healthy controls and patients with ibm, fshd and opmd," *J Neuromuscul Dis* **7**(4), 495–504 (2020).

[7] Naarding, K. J., Reyngoudt, H., van Zwet, E. W., Hooijmans, M. T., Tian, C., Rybalsky, I., Shellenbarger, K. C., Le Louër, J., Wong, B. L., Carlier, P. G., Kan, H. E., and Niks, E. H., "Mri vastus lateralis fat fraction predicts loss of ambulation in duchenne muscular dystrophy," *Neurology* **94**(13), e1386 (2020).

[8] Warman Chardon, J., Díaz-Manera, J., Tasca, G., Bönnemann, C. G., Gómez-Andrés, D., Heerschap, A., Mercuri, E., Muntoni, F., Pichiecchio, A., Ricci, E., Walter, M. C., Hanna, M., Jungbluth, H., Morrow, J. M., Fernández-Torrón, R., Udd, B., Vissing, J., Yousry, T., Quijano-Roy, S., Straub, V., and Carlier, R. Y., "Myo-mri diagnostic protocols in genetic myopathies," *Neuromuscul Disord* **29**(11), 827–841 (2019).

[9] Keene, K. R. and van Vught, L., "The feasibility of quantitative mri of extra-ocular muscles in myasthenia gravis and graves orbitopathy," **34**(1), e4407 (2021).

[10] Sproule, D. M., Montgomery, M. J., Punyanitya, M., Shen, W., Dashnaw, S., Montes, J., Dunaway, S., Finkel, R., Darras, B., Vivo, D. C. D., and Kaufmann, P., "Thigh muscle volume measured by magnetic resonance imaging is stable over a 6-month interval in spinal muscular atrophy," *Journal of Child Neurology* **26**(10), 1252–1259 (2011).

[11] Ma, J., "Dixon techniques for water and fat imaging," *Journal of Magnetic Resonance Imaging* **28**(3), 543–558 (2008).

[12] Fischmann, A., Hafner, P., Fasler, S., Gloor, M., Bieri, O., Studler, U., and Fischer, D., "Quantitative mri can detect subclinical disease progression in muscular dystrophy," *Journal of Neurology* **259**(8), 1648–1654 (2012).

[13] Charles, J. P., Suntaxi, F., and Anderst, W. J., "In vivo human lower limb muscle architecture dataset obtained using diffusion tensor imaging," *PLOS ONE* **14**(10), e0223531 (2019).

[14] Monte, J. R., Hooijmans, M. T., Froeling, M., Oudeman, J., Tol, J. L., Maas, M., Strijkers, G. J., and Nederveen, A. J., "The repeatability of bilateral diffusion tensor imaging (dti) in the upper leg muscles of healthy adults," *European Radiology* **30**(3), 1709–1718 (2020).

[15] Fedorov, A., Beichel, R., Kalpathy-Cramer, J., Finet, J., Fillion-Robin, J.-C., Pujol, S., Bauer, C., Jennings, D., Fennessy, F., and Sonka, M., "3d slicer as an image computing platform for the quantitative imaging network," *Magnetic resonance imaging* **30**(9), 1323–1341 (2012).

[16] Jared, R. H. F., "Total knee replacement," (2020). https://orthoinfo.aaos.org/en/treatment/total-knee-replacement/.

[17] Simpson, A. H. R. W., Howie, C. R., Kinsella, E., Hamilton, D. F., Conaghan, P. G., Hankey, C., Simpson, S. A., Bell-Higgs, A., Craig, P., Clement, N. D., Keerie, C., Kingsbury, S. R., Leeds, A. R., Ross, H. M., Pandit, H. G., Tuck, C., and Norrie, J., "Osteoarthritis preoperative package for care of orthotics, rehabilitation, topical and oral agent usage and nutrition to improve outcomes at a year (opportunity); a feasibility study protocol for a randomised controlled trial," *Trials* **21**(1), 209 (2020).

[18] Taha, A. A. and Hanbury, A., "Metrics for evaluating 3d medical image segmentation: analysis, selection, and tool," *BMC medical imaging* **15**(1), 29 (2015).

[19] Azimbagirad, M., Simozo, F. H., Senra Filho, A. C. S., and Murta Junior, L. O., "Tsallis-entropy segmentation through mrf and alzheimer anatomic reference for brain magnetic resonance parcellation," *Magnetic Resonance Imaging* **65**, 136–145 (2020).

[20] Wokke, B. H., Bos, C., Reijnierse, M., van Rijswijk, C. S., Eggers, H., Webb, A., Verschuuren, J. J., and Kan, H. E., "Comparison of dixon and t1-weighted mr methods to assess the degree of fat infiltration in duchenne muscular dystrophy patients," *Journal of Magnetic Resonance Imaging* **38**(3), 619–624 (2013).

[21] Van Griethuysen, J. J., Fedorov, A., Parmar, C., Hosny, A., Aucoin, N., Narayan, V., Beets-Tan, R. G., Fillion-Robin, J.-C., Pieper, S., and Aerts, H. J., "Computational radiomics system to decode the radiographic phenotype," *Cancer research* **77**(21), e104–e107 (2017).

[22] Faria, V. D. A., Azimbagirad, M., Arruda, G. V., Pavoni, J. F., Felipe, J. C., Junior, L. O. M., et al., "Prediction of radiation-related dental caries through pyradiomics features and artificial neural network on panoramic radiography," *Journal of Digital Imaging* , 1–12 (2021).

Table 3. Results of abnormality detection using Texture-Shape-Diffusivity metrics and reference scores for 4 patients. Patients are defined as P_{ij}, where i=number of patient and j=number of acquisition, A=abnormal, N=normal, /= not acquired

Subjects	Protocol	VM	VI	VL	RF	SM	ST	BSH
P_{11}	DIXON	A	A	N	A	A	A	N
	DTI	N	N	N	N	A	N	A
	T2 mapping	A	N	A	A	A	A	A
	T1 mapping	A	A	A	N	A	N	A
P_{12}	DIXON	A	N	N	A	A	A	N
	DTI	N	N	N	A	N	N	N
	T2 mapping	A	N	A	A	A	A	N
	T1 mapping	A	A	N	N	A	A	A
P_{13}	DIXON	A	A	A	A	A	A	N
	DTI	/	/	/	/	/	/	/
	T2 mapping	/	/	/	/	/	/	/
	T1 mapping	/	/	/	/	/	/	/
P_{21}	DIXON	A	A	N	A	A	A	N
	DTI	N	N	A	N	N	N	A
	T2 mapping	A	N	A	N	A	A	N
	T1 mapping	A	N	A	N	A	A	N
P_{22}	DIXON	A	A	A	A	N	N	N
	DTI	N	A	A	N	A	A	A
	T2 mapping	A	N	A	A	A	A	N
	T1 mapping	N	N	A	N	A	A	N
P_{23}	DIXON	A	A	A	A	A	N	N
	DTI	A	N	N	N	A	N	N
	T2 mapping	A	A	A	A	A	A	N
	T1 mapping	A	A	A	A	A	A	N
P_{31}	DIXON	N	N	N	A	N	N	N
	DTI	A	N	N	N	N	N	A
	T2 mapping	N	N	N	A	N	N	A
	T1 mapping	A	N	N	A	A	N	N
P_{32}	DIXON	A	N	N	A	A	N	N
	DTI	N	N	N	N	N	N	A
	T2 mapping	N	N	N	N	A	N	A
	T1 mapping	A	A	N	A	N	A	A
P_{33}	DIXON	A	A	A	A	N	A	N
	DTI	N	N	N	N	A	N	A
	T2 mapping	N	N	N	N	N	N	A
	T1 mapping	A	A	N	A	A	N	N
P_{41}	DIXON	A	A	A	A	N	A	N
	DTI	N	N	N	N	A	N	N
	T2 mapping	A	A	N	A	A	A	N
	T1 mapping	A	A	A	A	A	N	A
P_{42}	DIXON	A	A	N	A	A	A	N
	DTI	N	N	N	A	N	N	A
	T2 mapping	A	A	N	A	A	A	A
	T1 mapping	N	N	N	A	A	N	A
P_{43}	DIXON	A	A	A	A	A	A	N
	DTI	A	A	N	A	A	A	N
	T2 mapping	A	A	N	A	A	A	N
	T1 mapping	A	A	A	A	A	A	A